Electronic supporting information for:

Ru-assisted synthesis of {111}-faceted Pd truncated bipyramids: a highly reactive, stable and restorable catalyst for formic acid oxidation

Dongshuang Wu, Minna Cao and Rong Cao*

State Key Laboratory of Structural Chemistry, Fujian Institute of Research on the Structure of Matter, Chinese Academy of Science, 155 Yangqiao West Road Fuzhou Fujian 350002 (P. R. China).

To whom correspondence should be addressed. E-mail: rcao@fjirsm.ac.cn

Experimental section

Chemicals and Reagents. Ethylene glycol (EG) and polyvinylpyrrolidone (PVP K-30, Mw=58000) were purchased from Sinopharm Chemical Reagent Co., Ltd. Ruthenium(III) chloride hydrate ($RuCl_3 \cdot xH_2O$) was purchased from Shanghai July Chemical Co., Ltd. Potassium tetrachloropalladate (II) (K_2PdCl_4) was obtained from Alfa Aesar. Pd-balck and Nafion solution (5 wt. %) were obtained from Aldrich. All the chemicals were used as received. Ultrapure water is used during

experiments (Millpore, 18.2MΩ cm).

Synthesis of {111}-faceted Pd truncated triangular bipyramids (TTBPs). $RuCl_3$ aqueous solution (3M, 0.08 ml) and K_2PdCl_4 aqueous solution (0.08 M, 3 ml) was introduced into EG solution (15 ml) contained PVP (0.05 g), which had been heated at 373 K under magnetic stirring in a capped vial. The reaction was allowed to proceed for 1 h. After collection by centrifugation with acetone and washed three times with water, the collected black product was dispersed in ethanol.

Chracterization. The morphologies of products were studied using JEOL-2010 and FEI Tecnai G20 transmission electron microscope (TEM). The sample for Inductively Coupled Plasma OES spectrometer (ICP) was performed on an Ultima 2 analyzer (Jobin Yyon). FTIR spectra are recorded with a spectral resolution of 2 cm^{-1} on an ABB Bomen MB102 IR spectrometer in the range 4000-400 cm^{-1}. X-ray photoelectron spectroscopy (XPS) was performed on a ULVAC PHI Quantera microprobe. For testing if there is any metallic Ru(0) at the initial stage of the reaction (t = 40 s), we dropped several drops of the reaction mixture onto the polished single-crystal silicon-chip. Before drying in a vacuum oven at r.t., the silicon-chip was purged with high pure N_2 to clear the EG, soluble Ru-species and PVP. Finally, the residual species on the silicon-chip was tested for XPS. The TTB Pd NPs were dried in vacuum oven at r.t. to obtain powder. Binding energies were calibrated

by setting the measured BE of C 1s to 284.65 eV, and Si 1p to 101.09 eV for TTB Pd NPs and metallic Ru(0), respectively. Electrochemical measurements were conducted on Epslion EC-2000 (BASi, America) analyzer.

Electrochemical measurement. Firstly, an ethanol dispersion of NPs colloid was mixed and stirred with carbon black for 48 h to give Pd/C catalysts. Based on the ICP analysis, the Pd loading was kept 10 wt. % of all samples. 3 μL of as-prepared catalysts aqueous suspension (1 mg_{Pd} mL^{-1}) was deposited on a modified glassy carbon electrode (3 mm in diameter). The solvent was allowed to evaporate at r.t. Then 4 μL dilute Nafion (0.02 wt. % in ethanol) was coated on the surface of catalysts and dried at r.t. Ag/AgCl electrode and Pt wire are used as a reference electrode and a counter electrode, respectively. Commercial Pd black (2 mg_{Pd} mL^{-1}, 3 μL) were employed as control group catalyst. All the electrolyte solutions were deaerated with high-purity nitrogen gas for 30 minutes. The Electrochemically active surface area (ECSA) calculated from the metal oxides reduction area was used to normalize the original CVs. All electrochemical experiments were performed at r.t. (22±1°).

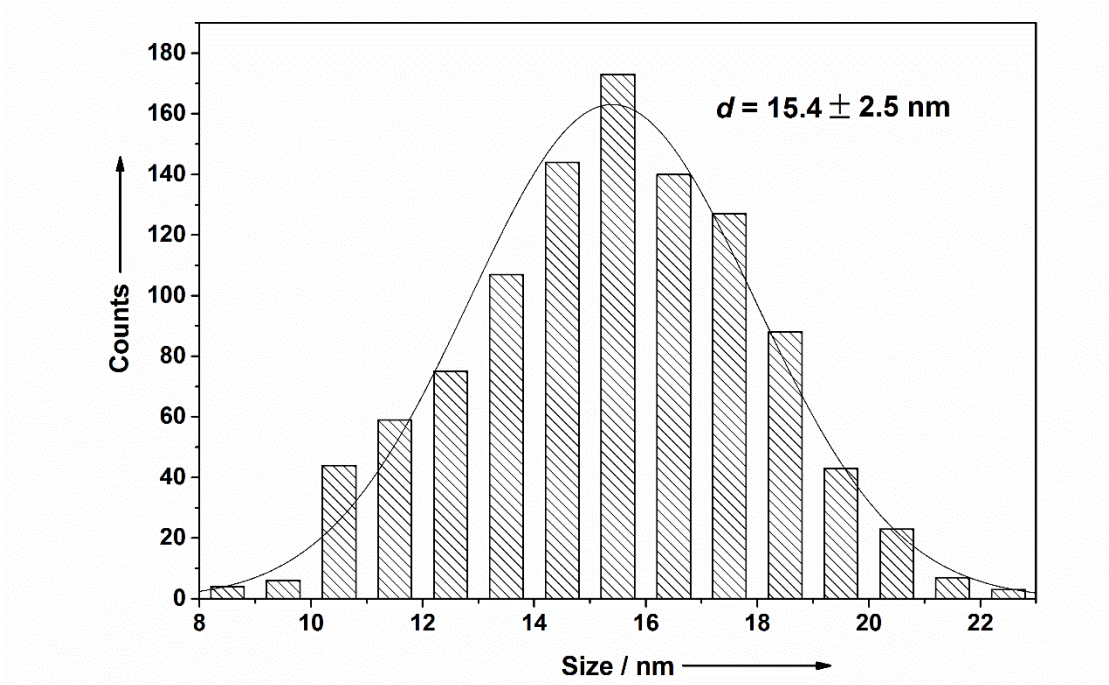

Fig. S1 size-distribition histogram of the TTBPs (obtained by counting at least 1000 nanoparticles).

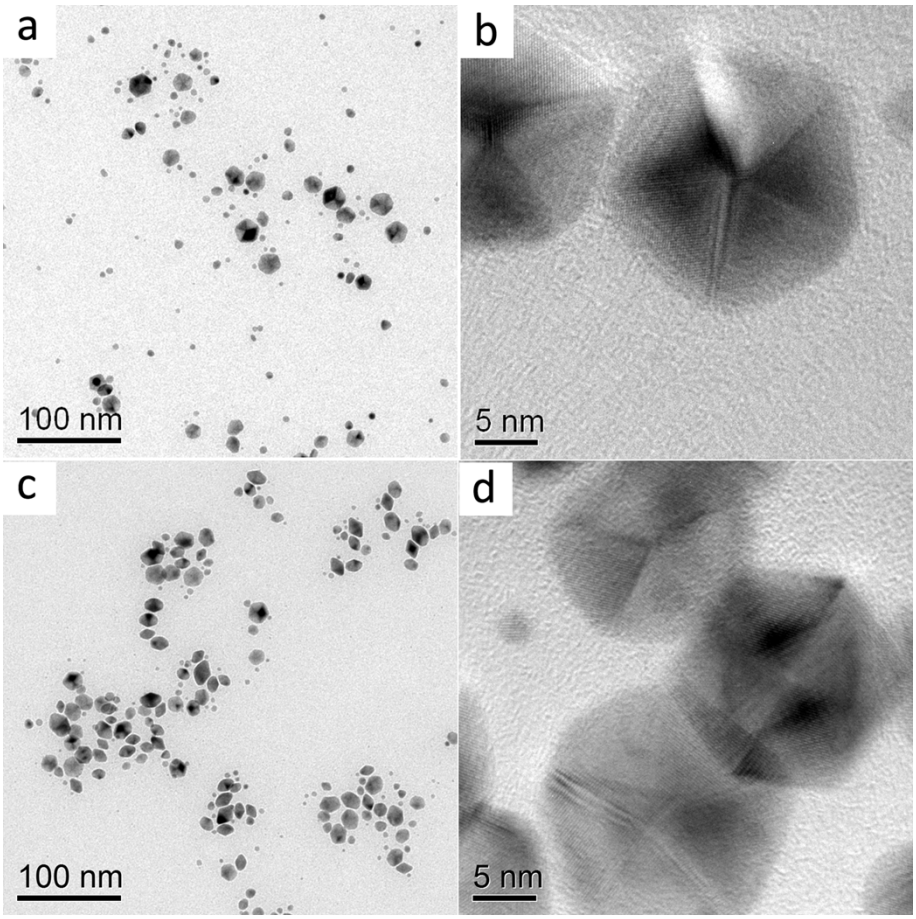

Fig. S2 TEM and HRTEM images of Pd decahedrons prepared under a

simlilar condtions with the standard process, except a) without the precense of $RuCl_3$, b)adding $RuCl_3$ after the nucleation of Pd.

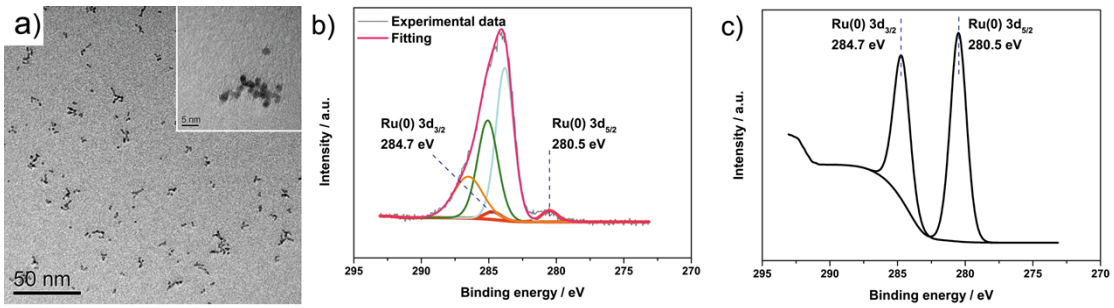

Fig. S3 Characterizations of sampled captured at t = 40 s. a) TEM images, inset is the corresponding HRTEM images. b) XPS curves shows Ru_{3d} photoemission, c) the enlarged fitting spectrum of Ru_{3d} photoemission in Fig. S2b.

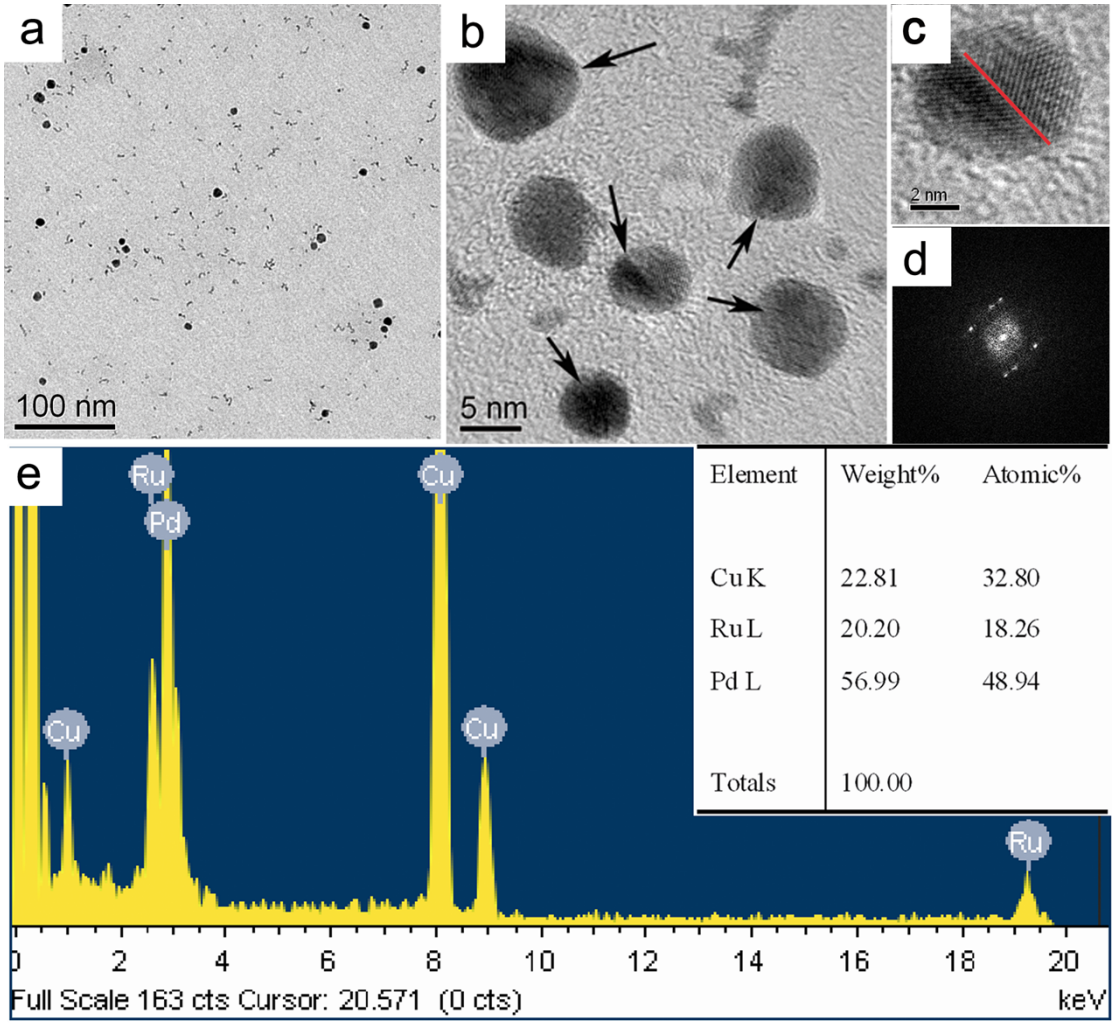

Fig. S4 Characterizations of sampled captured at t = 5 min. a) Large area TEM images, b) HRTEM images, the black arrows indicate the twinned boundaries, c) the HRTEM images and d) the corresponding Fast Fourier Transformation (FFT) pattern of an optional NPs in Fig. S4b, the red line suggests the presence of single-twinned plane, e)corresponding EDX spectra of the sample captured t = 5 min indicated that single-twinned Pd structures are coexist with Ru clusters.

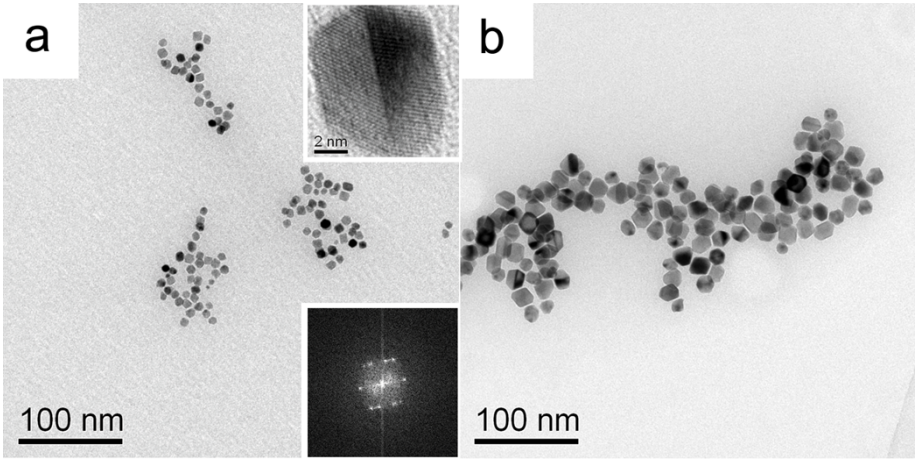

Fig. S5 TEM images of the TTBPs captured at a) 40 min, insets are a representive HRTEM image of an optional NPs and the corresponding FFT image; b) 3 h, respectively.

It worth noting that at the initial stage, the EG, PVP and $RuCl_3$ mixture went through a sequence of colour change within 40 s, which was from reddish brown to pale light green and then almost colourless. TEM image along with XPS analysis (Fig. S3, ESI†) shows the foramtion of ultra-small Ru(0) branched cluster at t = 40 s. With the addition of K_2PdCl_4 aqueous, the mixture colour changed slowly into light brown within 5 min. In sharp contrast with the burst nucleation in control groups (Fig. S2, ESI†), such a slow nucleation suggests a different nucleation pathway. Large-area TEM image and the corresponding EDS analysis at t= 5 min indicate that Pd structures coexist with Ru clusters (Fig. S4a and e, ESI†). These Pd structures are uniformly dispersed, characterized of rougher boundary and surface, and of about 5 nm in size. The representative HRTEM images and the corresponding 2-fold streaking FFT pattern further indicate the single-twinned nature (Fig. S4b-d, ESI†). As the reaction continues, the Ru clusters gradually disappear and the anisotropic and epitaxial growth of single-twinned Pd structures continues. The morphology of Pd NPs at t = 40 min (Fig. S5a, ESI†) shows well-faceted TTBPs with smooth surfaces, distinct single-twinned planes and increased particle size. Beyond 1 h, neither the size nor structure has significant change up to 3 h (Fig. S5b, ESI†).

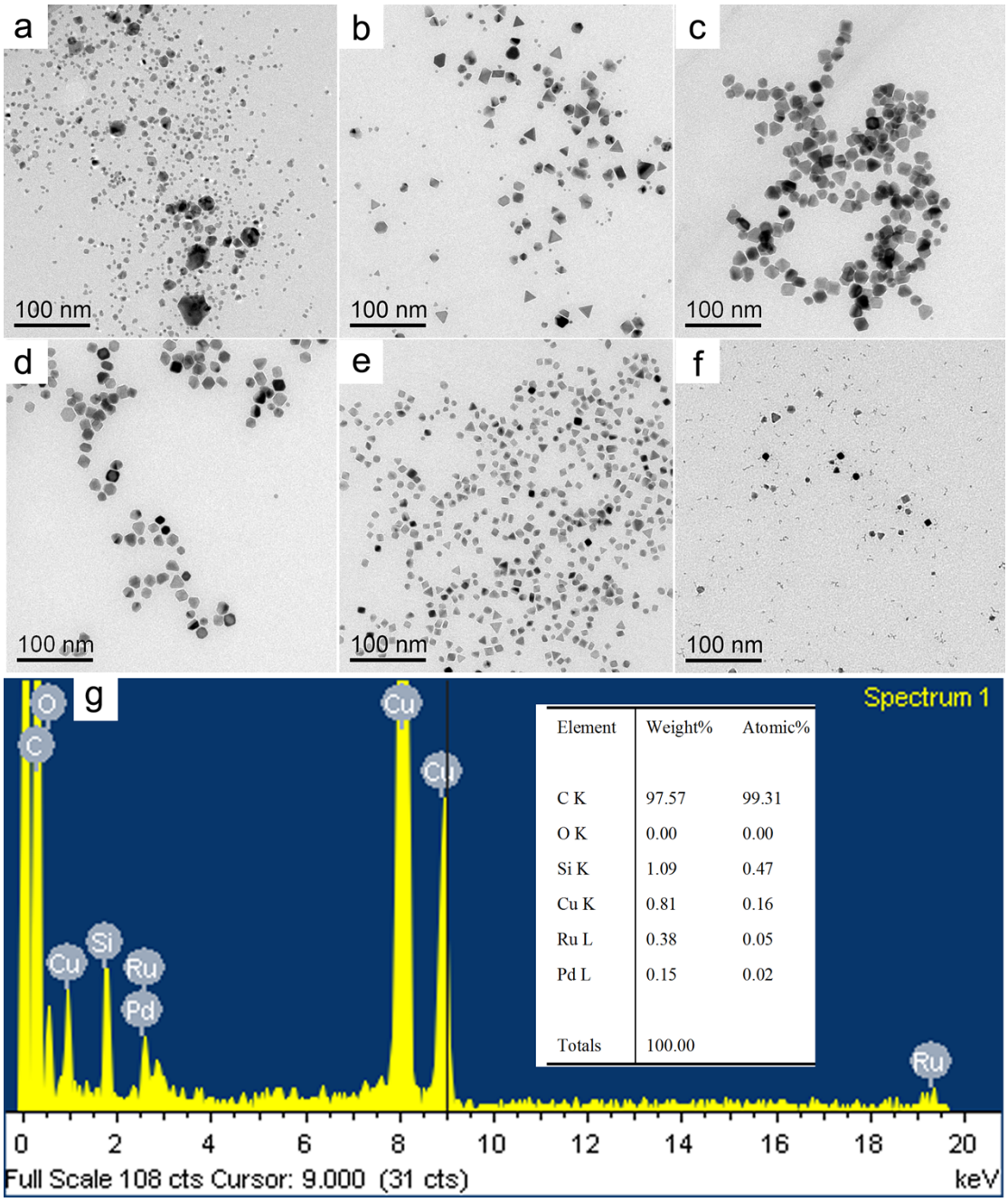

Fig. S6 TEM images of samples obtained at a varied concentration of $RuCl_3$ aqueous solution, a) 0.03 M, b) 0.3 M, c) 0.6 M, d) 1.5 M, e) 6 M, f) 15 M; g) the corresponding EDS analysis of the sample in Fig S6f. The volume of the aformentioned $RuCl_3$ aqueous solution added into the raction was fixed at 0.08 ml with the standard synthetic proceedure.

It is clearly that the amount of $RuCl_3$ in the reaction solution played a critical role in the formation of TTBPs. Figure S6a shows TEM image of the as-prepared sample

when a 100 times reduced amount of $RuCl_3$ (0.03 M, 0.08 ml) was added to the reaction solution. In this case, irregular shaped Pd NPs were obtaied with a rare exception of a few single-twinned NPs and with a large size distribution varying in the range of 3-50 nm. This can be explained by the insufficient Ru(0) formation in the early stage of the reaction. With increasing amount of $RuCl_3$ to 0.3 M, the number of TTBPs gradually increase with about 70% purity along with a narrower size distribution (Fig. S6b). When the concentration of $RuCl_3$ is in the range of 0.6 M-6 M, we obtained TTBPs with almost 90% purity (Fig. S6c-e). It worth noting that the average size of the as-obtained NPs are decreasing from 16.5 nm, 13.8 nm to 9.9 nm, repectively, with the increasing of amount of $RuCl_3$. It can be attributed to the increasing of amount of Ru(0) clusters can lead to increasing amount of single-twinned Pd stuctures. The amount of K_2PdCl_4 used to epitaxial growth, however, are decreasing when the dosing of added K_2PdCl_4 precursor is fixed for all cases, and thus leading to a samller size of Pd NPs in the end. When the amount of $RuCl_3$ added into the reation was increased to 15 M, Pd NPs are co-existed with the branched Ru NPs as shown in Fig. S6f. Such result also can be testified by the corresponding EDS analysis in Fig. S6g. This might be due to the amount of Ru(0) clusters is a lot excess over the stoichiometric ratio of the GRR. Therefore, the optimal amount of $RuCl_3$ for producing TTBPs should be in the range of 0.3-6 M.

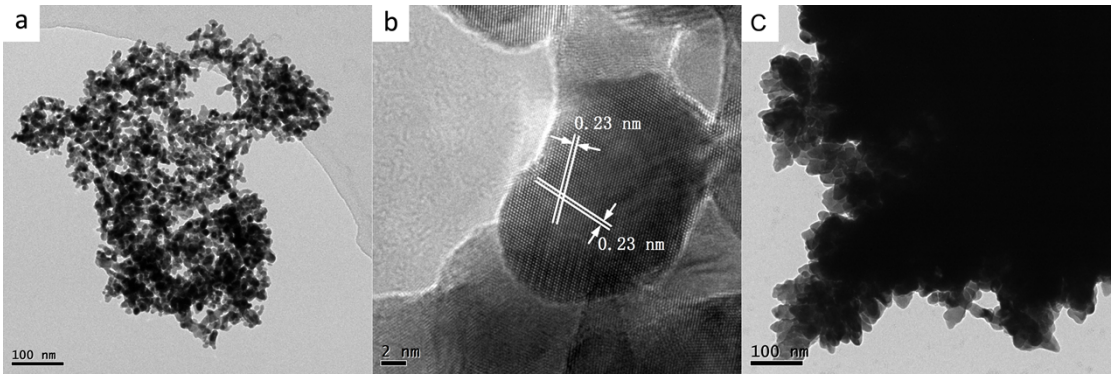

Fig. S7 a) TEM and b) HRTEM images of commercial Pd black catalysts fresh from Sigma-Aldrich company, c) TEM images of commercial Pd black catalysts after degradation test.

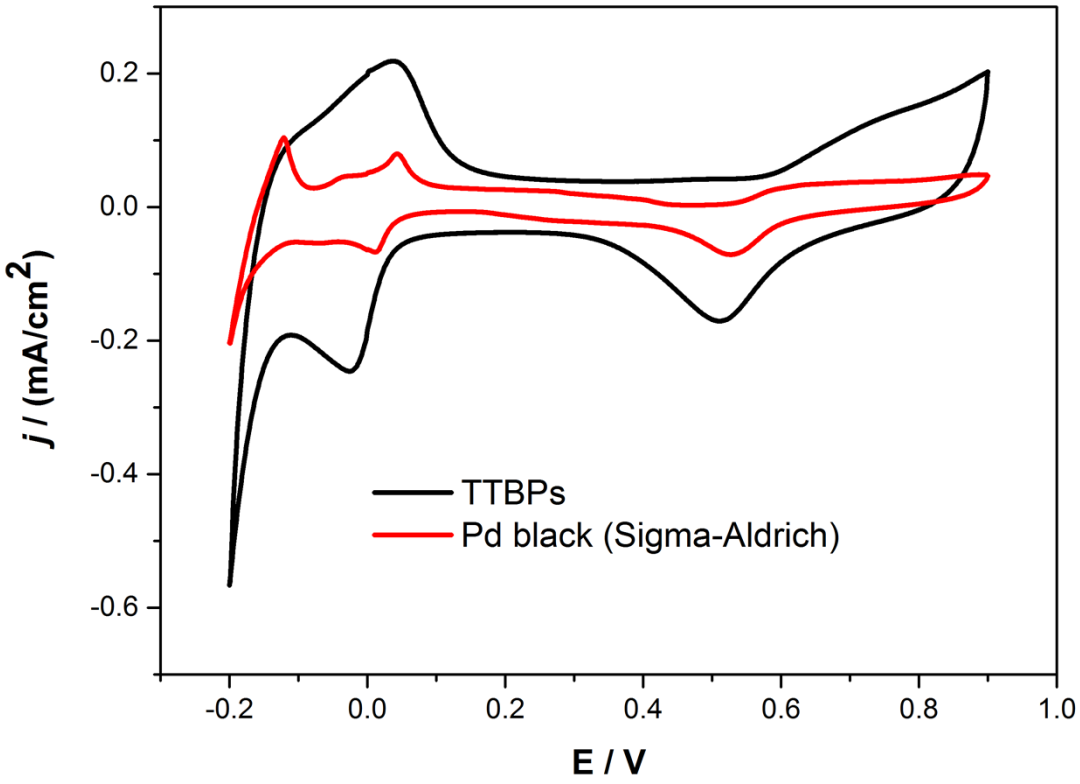

Fig. S8 CVs of TTBPs and Pd black in N_2-purged 0.5 M H_2SO_4. Scan rate: 50 mV s^{-1}.

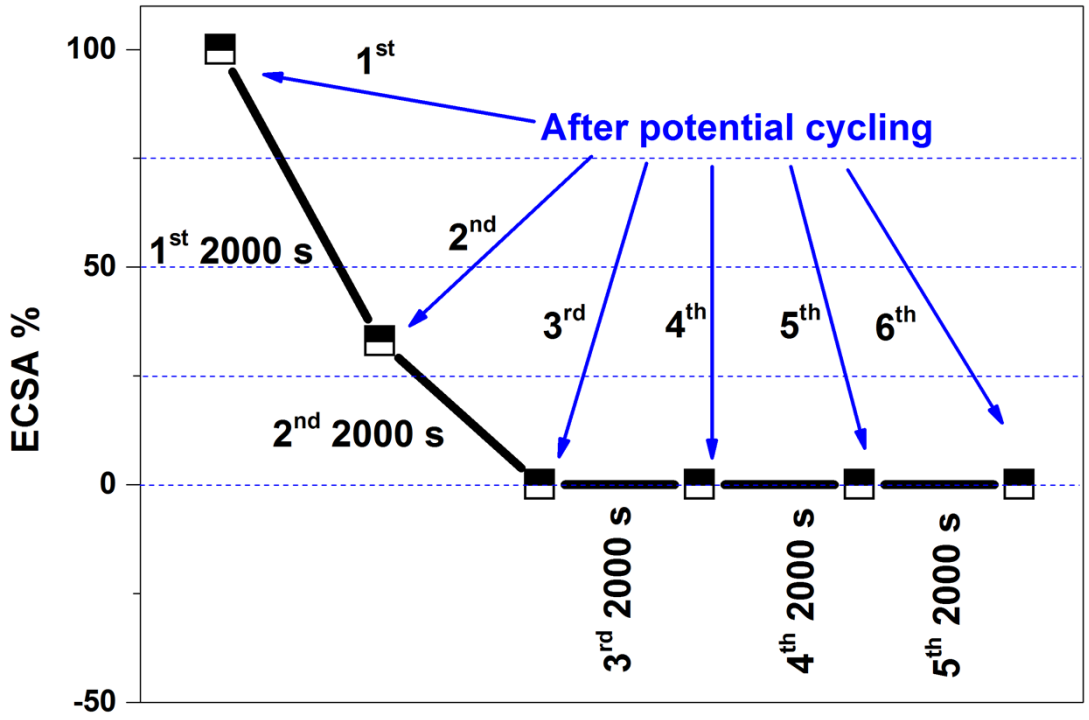

Fig. S9 degradation curves, ECSA% of commerical Pd black after each 200 potential cycles in N_2-saturated 0.5 M H_2SO_4. After the 1st, 2nd, …and 5th 200 potential cycles, the DC potential amperometry (DCPA) technique was conducted for formic acid oxidation at 0.2 V in 0.5 M H_2SO_4 + 0.25 M HCOOH solution for 2000 s, respectively. The ECSAs were calculated with respect to that of the 1st 200 potential cycles, respectively. Scan rate: 50 mV s^{-1}.

Since 6 μg of commerical Pd black cannot withstand the first 200 potential cycling, catalyst loading on the GC electrode is 16 μg in this case. The ECSA only preserve 33.2% of the initial value at the 2nd point. At the 3rd point, there is only 0.7% left. From the 4th point, the ECSA value decrease by three and four orders of magnitude. In sharp contrast, the TTBPs still perseves its inintal ECSA at the 6th point as shown in the main text.

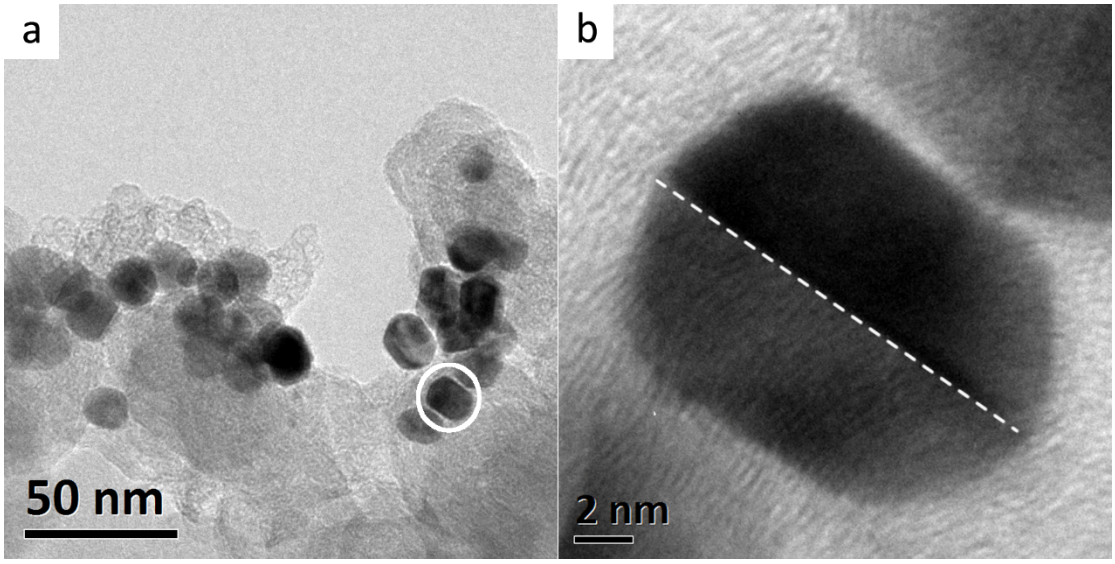

Fig. S10 (a) TEM images of TTBPs after degradation test. (b) The corresponding HRTEM image of the TTBP marked by a white circle, from which the twin boundary can be seen clearly as indicated by the white dash line.

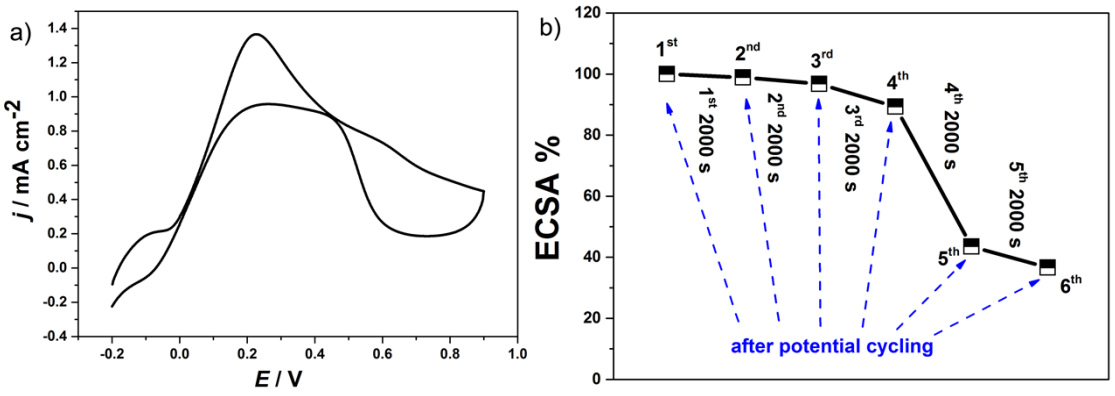

Fig. S11 a) CVs of 5-fold twinned Pd decahedrons obtained in 0.5 M H_2SO_4 + 0.25 M HCOOH solution. b) Degradation curves, ECSA% of 5-fold twinned Pd decahedrons after each 200 potential cycles in N_2-saturated 0.5 M H_2SO_4. The 5-fold twinned Pd decahedrons were obtained in

control group, which was manuiplated under the condition with out the addition of $RuCl_3$ as shown in Fig. S2a and b.

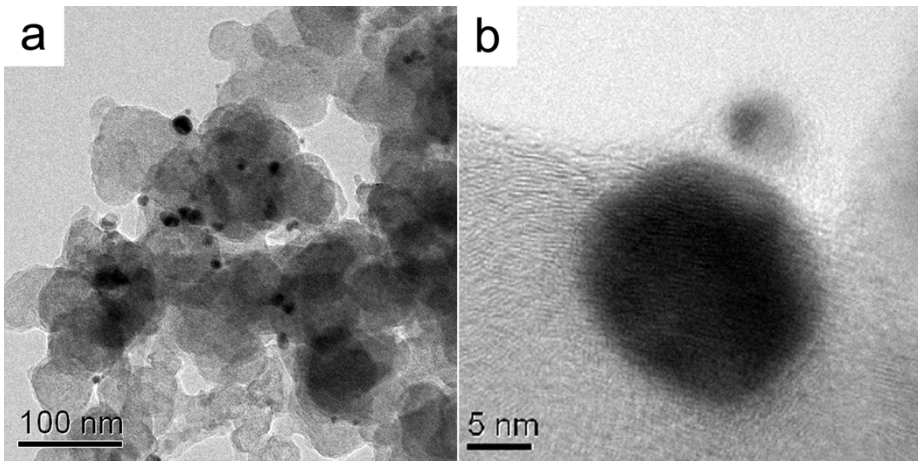

Fig. S12 a) TEM and b) HRTEM images of the 5-fold twinned Pd decahedrons after degradation test. Compared with their original TEM and HRTEM images as shown in Fig. S2a and b, it is obvious that the 5-fold multiply-twinned boundaries almost disappear after degradation test.

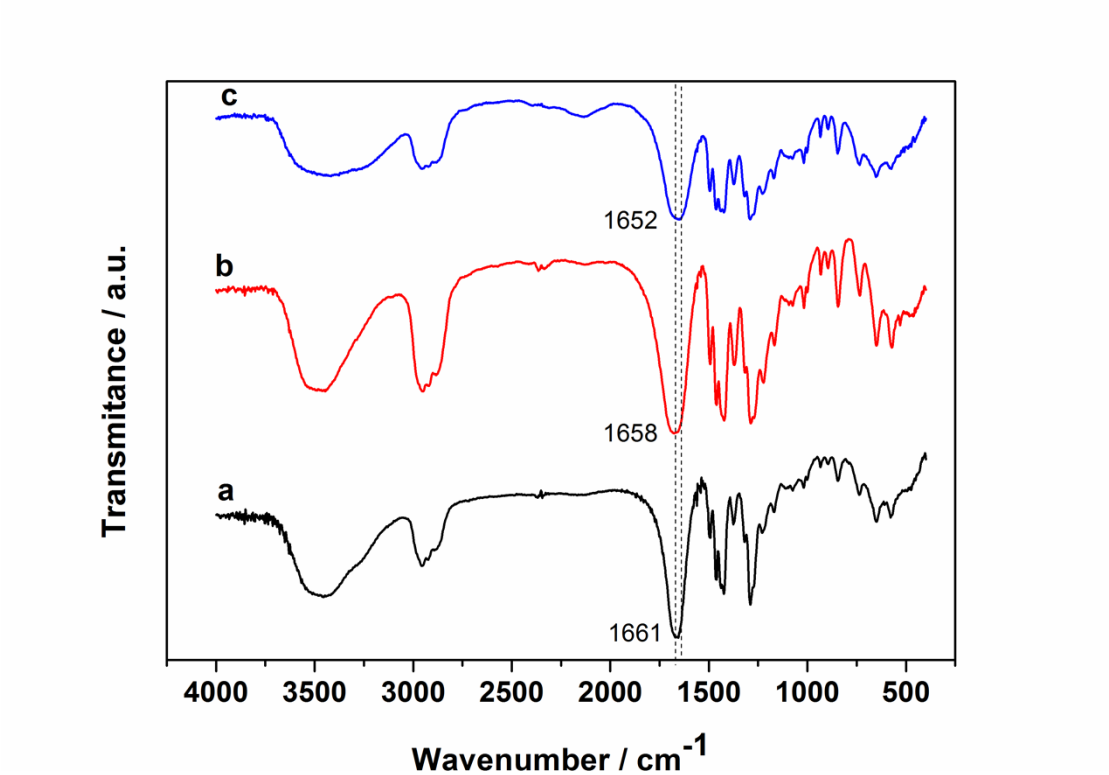

Fig. S13 FTIR spectra of the a) pure PVP. b) 5-fold twinned Pd decahedrons. c) the as-prepared TTBPs.

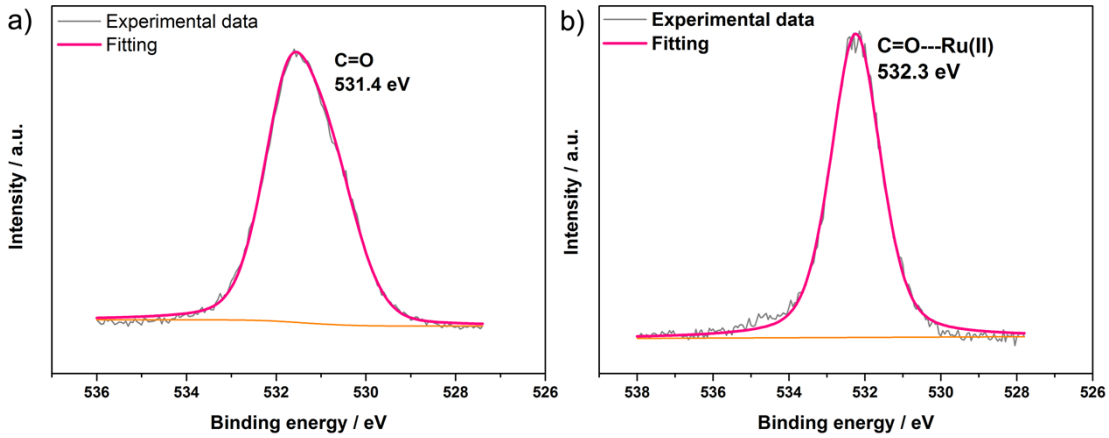

Fig. S14 XPS curves of O_{1S} photoemission in a) 5-fold twinned Pd decahedrons, b) TTBPs

As shown in Fig. S11a, the forward peak current density of 5-fold twinned Pd decahedrons is 1.36 mA cm^{-2}, which is only one-half of that of TTBPs. After the degradtion test, their initial ECSA only has 36% left as shown in Fig. S11b. TEM and HRTEM images in Fig. S12 further demonstrate that the tiwnned planes have

disappeared after the degadation test. The weaker antioxidant capacity of multiply-twinned stuctures than that of single-twinned structures may be one reason leading to such bad durability of decahedrons.

In view of catalytic activity, however, the multiply-twinned morphorlogy of these decahedrons should be more active towards formic acid oxidation than TTBPs because they expose more corner and edge atoms than single-twinned NPs. But the fact that the 5-fold twinned decahedrons are not acturally like that. Similar to TTBPs, 5-fold twinned Pd decahedrons are also {111}-faceted nanoparticles apart form the surface-adsorbed Ru(II) species. Therefore, it can speculate that the surface-adsorbed Ru(II) species may lead to an enhancement on the catalytic activity of the TTBPs.

FTIR spectra and XPS curves were used to give further information about the surface-adsorbed Ru(II) species. As shown in Fig. S13, for pure PVP molecules, a typical transmitted peak at ν_{max}/cm^{-1} 1661 is clearly observed, arising from the stretching vibration of C=O.[1] A slight red shift around 3 cm^{-1} is observed in the corresponding band for 5-fold twinned Pd decahedrons (1658 cm^{-1}), indicating a interaction of the PVP carbonyl group to the surface Pd atom.[2] In a sharp comparsion, the C=O of the TTBPs sample has a strong red shift of 9 cm^{-1}, suggesting that a interaction between Ru(II) and the C=O of PVP and the C=O is becoming softer in the TTBPs assembly. This effect can be attributed the electron-donation from the electron-rich carbonyl portal to Ru(II),[3] weakening the C=O bond. In consistent with the FTIR analysis, the XPS curves of O_{1S} photoemission also indicate that in TTBPs the surface-adsorbed Ru(II) has a interaction with C=O from PVP molecules. As shown in Fig. S14, for 5-fold twinned Pd decahedrons, the O_{1s} in C=O has a peak at 531.3 eV, which is similar to pure PVP molecules.[4] As a comparison, the corresponding energy in the TTBPs shifts to 532.3 eV (Fig. 2b), indicating an electron transfer from C=O to Ru(II). The atomic percentage of Ru(II) is 0.6% revealed by ICP. In contrast, the semi-quantitative result of XPS analysis shows that the percentage of Ru can reach 30 %. Such results suggest that Ru(II) are enriched on the surface of the formed TTBPs by interacting with with the surfcant PVP.

In theory, the surface-adsorbed Ru(II) can provide more favorite items for TTBPs' application in electrocatalysis. First, the interaction between Ru(II) and PVP weakens the protecting ability of PVP to expose more active sites on Pd surface and consequently enhances the activity. Second, the Ru(II)-PVP species can act as a unique capsule protecting the Pd atoms from migrating and aggregating. And thus, the TTBPs demonstrate much more enhanced catalytic performance than 5-fold twinned Pd decahedrons.

References

1. K. Chan, L. E. Kostun, W. E. Tenhaeff and K. K. Gleason,

Polymer, 2006, **47**, 6941.

2. Y. Borodko, S. E. Habas, M. Koebel, P. Yang, H. Frei and G. A. Somorjai, *J. Phys. Chem. B* 2006, **110**, 23052.
3. T. C. Lee and O. A. Scherman, *Chem. Commun.*, 2010, **46**, 2438.
4. B. D. Beamson G., *High Resolution XPS of Organic Polymers: the Scienta ESCA300 Database*, 1992.